Influence of the Substitution of Manganese for Iron in the Fe₄N Lattice on Particle Formation and Magnetic Properties

B. SIBERCHICOT, S. F. MATAR, L. FOURNES, G. DEMAZEAU, AND P. HAGENMULLER

Laboratoire de Chimie du Solide du CNRS, Université de Bordeaux I, 351, cours de la Libération, 33405 Talence Cedex, France

Mössbauer resonance studies on Mn-substituted Fe₄N show that manganese occupies statistically both iron sites in the lattice. Replacement of Fe by Mn modifies the crystal growth process of Fe₄N magnetic particles and leads to improvement of the extrinsic magnetic properties, i.e., H_c and σ_r/σ_s, required for magnetic recording applications. © 1990 Academic Press, Inc.

At present magnetic recording constitutes an important research area due to the fast-developing requirements of information storage as a consequence of more sophisticated uses of the computer. A number of specific characteristics may be required for relevant materials:

—specific morphology: submicrometer particles corresponding to magnetic monodomains, with a crystallite shape appropriate to the required recording technique;

—magnetic characteristics: high values of saturation magnetization (σ_s) of remanent magnetization (σ_r), and of σ_r/σ_s ratios on the one hand and a coercive field (H_c) high enough to be compatible with writing–recording techniques and erasing procedures (*1*) on the other hand.

Classical examples are the oxides derived from γ-Fe₂O₃ (*2*) or from CrO₂ (*3*) and metallic iron alloys (*4*). Recently Fe₄N has been the subject of intensive experimental (*5, 6*) and theoretical (*7*) studies. The interest in this nitride arises from the high value

of its saturation magnetization: 208 emu/g (extrapolated value at 0 K) (*8*), which is very close to that of pure α-Fe (218 emu/g). Moreover, as a fine powder Fe₄N presents a chemical resistance higher than that of metallic alloys in fine powder form to oxidation by air or water vapor. Partial substitution of carbon for nitrogen which occurs preferentially near the surface may enhance such a phenomenon (*9*).

To achieve better control of the size and the morphology of the magnetic particles, substitution of iron by tin has been studied using Mössbauer spectroscopy (*9*): tin substitutes preferentially for iron in one of two available sites, i.e., Fe$_I$ at the corner position, rather than Fe$_{II}$ at face centers (Fig. 1). This preference of Sn has been attributed to the size difference between Fe and Sn—the atomic radii being 1.17 and 1.40, respectively (*10*)—with respect to the larger size of site Fe$_I$ ($1.42 \leq r[\text{Fe}_I] \leq 1.55$ Å and $1.13 \leq r[\text{Fe}_{II}] \leq 1.27$ Å).

In order to distinguish this size effect from the influence of the electronic struc-
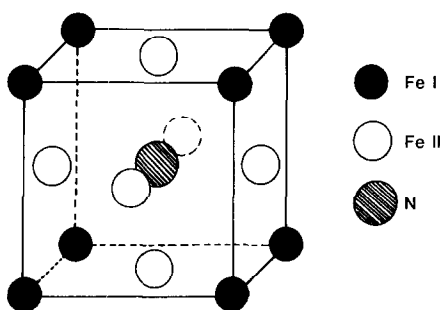
FIG. 1. Crystal structure of Fe$_4$N.

ture of the substituting element, it was relevant in a second step to investigate the substitution of iron by another element of similar size. The neighboring elements are Mn (Z_{Fe} + 1) with atomic radii $r_{Mn} \cong 1.17$ Å and $r_{Co} \cong 1.16$ Å, close to that of iron (1.17 Å). In this investigation we have carried out the study of the solid solutions Fe$_{4-x}$Mn$_x$N.

I. Experimental Procedure for the Preparation of Precursor and Magnetic Crystallites

I.1. Preparation of Oxalate Precursors

The substitution of Mn for Fe into the Fe$_4$N lattice can be achieved either by starting with a substituted precursor or by adding the substituent during the synthesis process of the magnetic material. The first alternative having been utilized, the procedure began with the precipitation of a mixed oxalate of iron and manganese [(Fe, Mn)C$_2$O$_4 \cdot$ 2H$_2$O] by reaction between aqueous solutions of oxalic acid and iron and manganese sulfates. The chemical conditions of pH and concentration were thoroughly studied (11). Fe- and Mn- oxalates of MC$_2$O$_4 \cdot$ 2H$_2$O formulation have orthorhombic and hexagonal symmetries, respectively (12). For Mn- substitution amounts up to 0.70 the X-ray diffraction patterns of the oxalates obtained by coprecipitation gave evidence of a unique phase

of orthorhombic symmetry. Because of the close values of the ionic radii of corresponding divalent ions (i.e., $r_{Mn^{2+}}$ = 0.80 Å and $r_{Fe^{2+}}$ = 0.74 Å (13)), only a slight increase in the unit cell volume could be detected (for instance: for x = 0, $V/Z \cong$ 131 Å^3 and for x = 0.70, $V/Z \cong$ 137 Å^3). We have shown the actual presence of Mn within the lattice by X-ray fluorescence using a STEM (scanning transmission electron micrograph) device.

I.2. Elaboration of the Magnetic Crystallites

The mixed nitrides were prepared by nitriding the corresponding oxalates Fe$_{1-y}$Mn$_y$C$_2$O$_4 \cdot$ 2H$_2$O; 0 < y < 0.25—such a composition range corresponding to to 0 < x < 1, i.e., x = 4y, for the nitride—using a *fluidized-bed* technique (6) at 400°C for 4 hr with a mixture of NH$_3$ and H$_2$ as gas vector. The experimental conditions required for obtaining a unique phase isostructural with Fe$_4$N are such that the ratio τ = NH$_3$/H$_2$ of the gas flow had to be reduced for increasing concentrations of Mn (from τ = 2.8 for y = 0 to τ = 2.1 for y = 0.225). This feature may involve an enhanced reactivity of the oxalate particles toward nitridization as x increases. This feature can be related to the higher thermodynamical stability of the substituted nitrides but is also likely to result from an enhanced reactivity of the oxalates. In the utilized procedure the experimental conditions depend largely on the specific area of the oxalate precursor (i.e., the particle size).

Partial substitution of nitrogen by carbon is to be expected for the Fe–Mn nitrides thus prepared. Actually, during thermal decomposition an oxalate gives off carbon monoxide which is in equilibrium with elemental carbon and carbon dioxide (14). This equilibrium gives rise to the carburizing conditions simultaneous with the existing nitriding conditions. The thermodynamic conditions used for the synthesis of

$Fe_{4-x}Mn_xN$ were close to those formerly adopted (14) starting from other oxalates; this material is likely to undergo an analogous substitution whereby nitrogen is partly replaced by carbon yielding a *carbo-nitride*: $Fe_{4-x}Mn_xN_{1-\varepsilon}C_\varepsilon$, $0 < x < 1$; $0.30 < \varepsilon < 0.8$.

The structure of Fe_4N is derived from that of γ-Fe (fcc). A substitution within the lattice which favors this structure is likely to lead to a substituted nitride. Manganese allows one to extend the existence of such a γ phase in iron-rich alloys (15), and hence favors the formation of the mixed nitrides of Fe_4N-type structure.

II. Structural and Morphologic Characterizations of the Mixed Fe–Mn Nitrides

II.1. X-Ray Diffraction

The X-ray diffraction patterns do not exhibit any significant modification of the cubic unit cell parameter of Fe_4N ($a = 3.797$ Å) (16). This result can be explained by the close sizes of both substituting elements as well as by the small values of x. The lattice parameter of isostructural Mn_4N is in fact 3.872 Å (16).

II.2. Mössbauer ^{57}Fe Resonance

The Mössbauer resonance spectrum of the substituted nitride for $x = 0.1$ at room temperature (293 K) is given in Fig. 2. It can be deconvoluted into three sextets and one central doublet (Table 1A). The parameters of each sextet are relatively close to those characterizing the nonsubstituted phase, i.e., Fe_4N (Table 1B).

Determining the ratio of the sums of intensities of the resonance lines (R_p) should identify a preferential substitution site for Mn. In fact, in Fig. 2, lines 1—at -5.24 mm/s—and 1'—at 5.68 mm/s—are relative to site (I) and lines 3—at -1.60 mm/s—and 3'—at 2.30 mm/s—are relative to site (II) (cf. Fig. 1). It must be stressed here that site (II) can be decomposed into two components $(II)_A$ and $(II)_B$; this is due to the electric field gradient at site (II). The ratio R_p is defined as: $R_p = (I_1 + I_{1'})/(I_3 + I_{3'})$, where I is the intensity of the peak referenced in index. Its value for the substituted phase (0.41) is very close to that previously determined for the nonsubstituted phase Fe_4N (0.45) (17). This result suggests that when x is large enough to make a difference, either manganese does not substitute for iron in Fe_4N (but this would be in contradiction with the X-ray fluorescence) or manganese has no significant site preference. This result is opposite to that obtained for $Fe_{4-x}Sn_xN$ ($x = 0.4$) where tin preferentially substitutes for iron at site Fe_I (i.e., $Fe_{II_3}Fe_{I_{1-x}}Sn_{I_x}N$). This seems to indicate the importance of the steric factor in

SPEED (mm s^{-1})

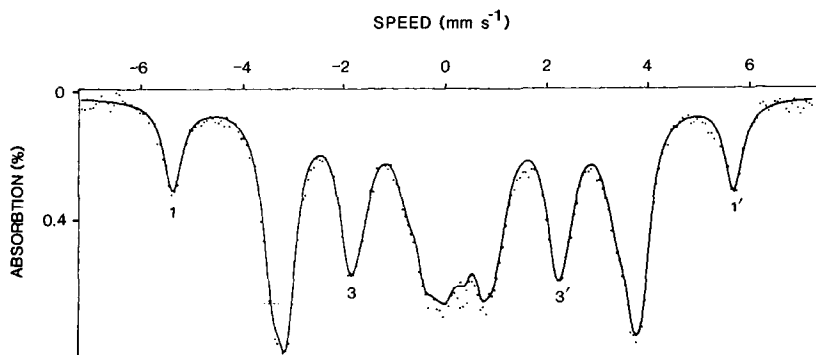FIG. 2. Mössbauer resonance spectrum of $Fe_{4-x}Mn_x(N, C)$ at 293 K for $x = 0.1$.

TABLE IA

Mössbauer Resonance Parameters of Fe$_{4-x}$Mn$_x$(N, C) (x = 0.1) at 293 K

	Hyperfine field H (T)	Isomer shift δ (mm/s)	Quadrupole perturbation (mm/s)		% obs.
Bulk					
Fe(I)	34.2 ± 0.2	0.22 ± 0.02	ε =	0.01 ± 0.02	25
Fe(II)$_A$	21.5 ± 0.2	0.33 ± 0.02	ε =	0.11 ± 0.02	43
Fe(II)$_B$	21.3 ± 0.2	0.32 ± 0.02	ε =	−0.12 ± 0.02	21
Fine grains					
Central doublet	—	0.26 ± 0.02	Δ =	0.34 ± 0.02	11

the substitutions of iron by other elements in Fe$_4$N.

The central doublet represents about 11% of the total iron content. As a matter of fact, in all substituted nitrides formerly studied—following the same preparation process—i.e., Fe–Sn, Fe–Ru, and Fe–Os (9, 17) there is an increasing percentage of total iron in the central doublet when the degree of substitution increases.

In these studies electron microscopy micrographs as well as the determination of the average size of the magnetic particle by the *X-ray Scherrer method* (18) pointed to a decrease in the size of grains to below the monodomain size ($\cong$ 150 Å) (Fig. 3 for Fe–Mn). For these systems as well as for those presently studied, this involves superparamagnetic behavior for the smallest crystallites. The high percentage observed in the case of the Fe–Mn–N system suggests that manganese plays a role in controlling the size of the magnetic grains.

III. Influence of the Substitution of Manganese for Iron on the Magnetic Properties of Fe$_4$N

Figure 4a shows the variation with x of the coercive field. The shape is similar to that previously observed for the tin substitution process (Fig. 4b (14, 17)).

The coercive field depends on two main factors: a geometric one (size and shape) and a magnetic one (magnetocrystalline effect) (19). It is well known that the spin-orbit coupling constant of Mn (195 cm^{-1}) is lower than that of Fe (275 cm^{-1}) (20). Consequently no enhancement of the magnetocrystalline anisotropy should be expected

TABLE IB

Mössbauer Resonance Parameters of Fe$_4$(N, C) at 293 K

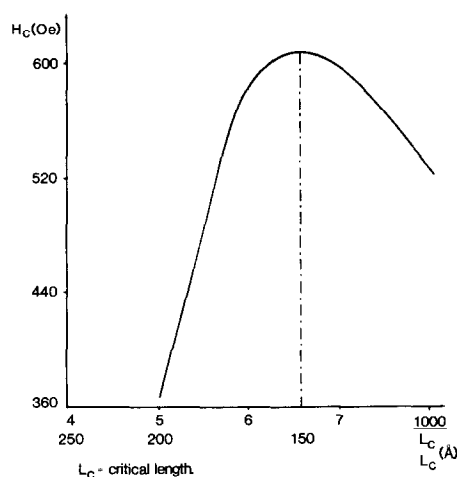|	Hyperfine field H (T)	Isomer shift δ (mm/s)	Quadrupole splitting ε (mm/s)
Fe(I)	34.0 ± 0.2	0.24 ± 0.02	0.00 ± 0.02
Fe(II)$_A$	21.2 ± 0.2	0.29 ± 0.02	0.10 ± 0.02
Fe(II)$_B$	21.2 ± 0.2	0.29 ± 0.02	−0.12 ± 0.02

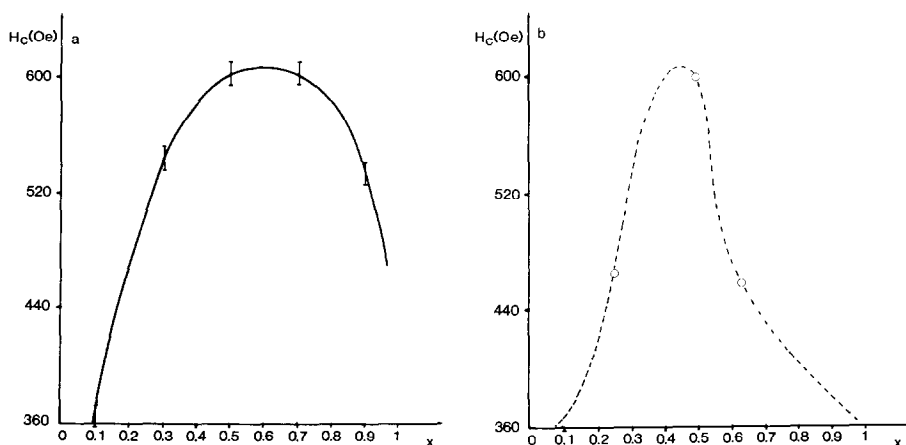Fig. 3. Variation of the coercive field of Fe$_{4-x}$Mn$_x$(N, C) as a function of the particle size.

FIG. 4. (a) Variation of the coercive field of $Fe_{4-x}Mn_x(N, C)$ as a function of composition x. (b) Variation of the coercive field of $Fe_{4-x}Sn_x(N, C)$ vs x.

with increasing substitution of Mn. This conclusion involves the shape of the $H_c = f(x)$ curve largely governed by the geometric factors characterizing the microcrystallites of $Fe_{4-x}Mn_xN$.

The shape of the average particle size distribution curve (Fig. 3) can be compared with that of the coercive field ($H_c = f(x)$; Fig. 4a). This suggests that the average size corresponding to magnetic monodomain particles ($\cong 150$ Å) is reached for $x \cong 0.6$. For even higher values of x the decreasing average size of the particles leads to an increasing number of small grains with superparamagnetic behavior.

Figure 5 indicates the improvement of the remanence ratio ($S = \sigma_r/\sigma_s$) for substitution amounts lower than 0.5; i.e., $S_{max.} \cong 0.4$.

σ_r may be considered an extrinsic property of the magnetic particles. For polydomain particles—after saturation of the samples and in the absence of magnetic field—the remanent magnetization is lower than that of the monodomain particles, due to the existence of nonaligned magnetic moments. This could explain the increase in the σ_r/σ_s ratio—which is hence an extrinsic property of the material—with the

decrease in particle size, i.e., with the tendency to formation of monodomains, at least for $x \cong 0.5$.

IV. Conclusion

The investigation of the substitution of manganese for iron in the Fe_4N lattice shows that this element can occupy without apparent preference both lattice sites. This result seems to illustrate, insofar as it can be related to previous observations for Sn
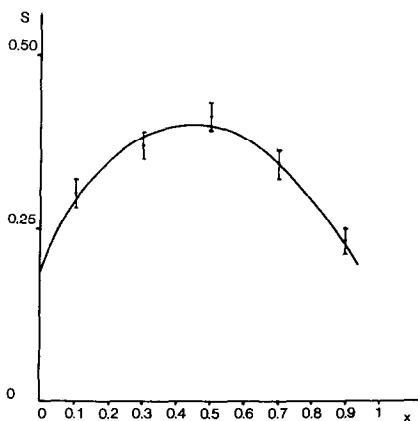

FIG. 5. Variation of the remanence S ($S = \sigma_r/\sigma_s$) of $Fe_{4-x}Mn_x(N, C)$ as a function of x.

substitutions, the predominant influence of size on the determination of the substitution site. Furthermore, despite random substitution, manganese plays an important role in determining the size of the magnetic crystallites during the nitride formation step. The important variation of the intrinsic magnetic properties with substitution gives further support to the actual substitution of Mn within Fe$_4$N. Therefore manganese is a valuable substituent: because of its particle size, it permits control over the magnitude of the coercive field as well as over the squareness of the hysteresis loop.

References

1. M. P. Sharrock and R. E. Bodnar, *J. Appl. Phys.* **57**(1), 3919 (1985).
2. P. Mollard, A. Collomb, J. Devenyi, A. Rousset, and J. Paris, *IEEE Trans. Magn. (MAG10)* **3**, 655 (1975).
3. G. Demazeau, P. Maestro, M. Pouchard, Th. Plante, and P. Hagenmuller, *Ann. Chim. (Paris)* **3**, 353 (1978).
4. A. L. Oppegard, F. J. Darnell, and H. C. Miller, *J. Appl. Phys.* **32**(3), 1845 (1961).
5. A. Tasaki, S. Harada, and T. Kusunose, *Proc. Int. Conf. Ferrites (Japan)*, 208 (1980).
6. G. Demazeau, D. Andriamandroso, M. Pou-
chard, B. Tanguy, and P. Hagenmuller, *C.R. Seances Acad. Sci. 2*, **297**, 843 (1983).
7. S. Matar, P. Mohn, G. Demazeau, and B. Siberchicot, *J. Phys.* **49**, 1761 (1988).
8. Ch. Guillaud and H. Creveaux, *C.R. Seances Acad. Sci.* **222**, 1170 (1946).
9. D. Andriamandroso, L. Fefilatiev, G. Demazeau, L. Fournes, and M. Pouchard, *Mater. Res. Bull.* **19**, 1187 (1984).
10. L. H. Ahrens, *Geochim. Cosmochim. Acta* **2**, 155 (1952).
11. B. Siberchicot, Thèse de docteur de l'Université de Bordeaux I (1989).
12. A. Hanawalt, *Anal. Chem.* **10**, 475 (1930).
13. R. D. Shannon, and C. T. Prewitt, *Acta Crystallogr. B* **25**, 925 (1969).
14. D. Andriamandroso, G. Demazeau, M. Pouchard, and P. Hagenmuller, *J. Solid State Chem.* **54**, 54 (1984).
15. A. Hellawell and W. Hume-Rothery, *Philos. Trans. R. Soc. London Ser. A* **249**, 417 (1957).
16. Ph. L'Heritier, D. Fruchart, R. Madar, and R. Fruchart in "Landolt-Börnstein Numerical Data and Functional Relationships in Science and Technology, New Series, Group 3: Crystal and Solid State Physics," Vol. 19c, part 2. Springer-Verlag, Berlin (1983).
17. D. Andriamandroso, Doctorate Thesis, University of Bordeaux I (1986).
18. Scherrer, "Zsigmondy Kolloïdchemie," 3rd ed., p. 387 (1920).
19. E. C. Stoner, and E. P. Wohlfarth, *Philos. Trans. R. Soc. London* **240**, 599 (1948).
20. J. Griffith, "The Theory of Transition Metal Ions," Cambridge Univ. Press, London/New York (1961).